BULLETIN OF THE POLISH ACADEMY OF SCIENCES
TECHNICAL SCIENCES, Vol. 70(4), 2022, Article number: e141725
DOI: 10.24425/bpasts.2022.141725

Anisotropy of structural and mechanical properties in CuCrZr alloy following hydrostatic extrusion process

Sylwia PRZYBYSZ*, Mariusz KULCZYK, Jacek SKIBA, and Monika SKORUPSKA

Institute of High Pressure Physics of the Polish Academy of Sciences, Warszawa, Poland

Abstract. The methods of severe plastic deformation (SPD) of metals and metal alloys are very attractive due to the possibility of refinement of the grains to nanometric sizes, which facilitates obtaining high mechanical properties. This study investigated the influence of SPD in the process of hydrostatic extrusion (HE) on the anisotropy of the mechanical properties of the CuCrZr copper alloy. The method of HE leads to the formation of a characteristic microstructure in deformed materials, which can determine their potential applications. On the longitudinal sections of the extruded bars, a strong morphological texture is observed, manifested by elongated grains in the direction of extrusion. In the transverse direction, these grains are visible as equiaxed. The anisotropy of properties was mainly determined based on the analysis of the static mini-sample static tensile test and the dynamic impact test. The obtained results were correlated with microstructural observations. In the study, three different degrees of deformation were applied at the level necessary to refine the grain size to the ultrafine-grained level. Regardless of the applied degree of deformation, the effect of the formation of a strong morphological texture was demonstrated, as a result of which there is a clear difference between the mechanical properties depending on the test direction, both by the static and dynamic method. The obtained results allow for the identification of the characteristic structure formed during the HE process and the more effective use of the CuCrZr copper alloy in applications.

Key words: hydrostatic extrusion; anisotropy; mechanical properties; grain refinement; CuCrZr alloy.

1. INTRODUCTION

Many current engineering applications require a combination of appropriate physical and mechanical properties [1]. The application of the severe plastic deformation (SPD) method in metals and metal alloys that have specific microstructural and design features may lead to high mechanical properties [2, 3]. It is related to the strong refinement of the microstructure to the ultrafine-grained (UFG) or nanocrystalline (NC) level [4–6].

The literature describes many SPD methods, thanks to which we can obtain the refinement of grains to nanometric or ultrafine grain size. Most of the literature data showing the influence of severe plastic deformations on the microstructure and properties of materials concern the following methods:

- Equal channel angular pressing (ECAP) [7, 8].
- High-pressure torsion (HPT) [9, 10].
- Accumulative roll Bonding (ARB) [11–13].
- Cyclic extrusion compression (CEC) [14].
- Hydrostatic extrusion (HE) [15–17].

The use of these methods allows us to increase the density of network defects, vacancies, and grain boundaries, and to obtain grain sizes of ≤ 100 nm [5].

Pure copper has excellent electrical properties, making it important for many areas of industry. However, its low mechanical strength limits its use considerably. In order to improve the mechanical strength of pure metals, many methods are used, for example, strain hardening, grain refinement, or solution hardening, which facilitates the formation of alloys by adding particles of the second phase. Unfortunately, each of these approaches negatively affects electrical conductivity. As a result, the CuCrZr copper alloy, which is an example of a combination of mechanical strength, and electrical and thermal conductivity, started to attract attention [18, 19]. The mechanical properties of this alloy are much higher compared to pure copper due to the addition of alloying elements enabling precipitation hardening.

High electrical conductivity is ensured by the low solubility of Cr and Zr in copper at room temperature [20–23]. Chromium and zirconium form an efficient alloying system for copper-based composition, which allows us to achieve the optimal combination of performance properties (mechanical strength and thermal conductivity). High electrical conductivity is achieved due to the low solubility of Cr and Zr in copper, while the high strength results from the precipitates and the precipitate enhancement mechanism. The combination of Cr and Zr in the copper matrix leads to the creation of a stable structure and the strengthening of copper with precipitates [24].

CuCrZr alloys are used, among others as spot welding electrodes and electric cables. Due to the combination of mechanical strength and good thermal conductivity, this alloy is considered a very good material for fusion reactor applications, e.g. the international thermonuclear experimental reactor (ITER) [25, 26]. These materials have the added benefit of

*e-mail: sylwia@unipress.waw.pl

Manuscript submitted 2022-04-12, revised 2022-06-02, initially accepted for publication 2022-06-03, published in August 2022.

being able to customize their properties through a variety of heat treatment and manufacturing processes to cover almost any known strengthening mechanism. The mechanical strength of CuCrZr while maintaining high electrical conductivity without changing the chemical composition can be obtained utilizing severe plastic deformation (SPD) techniques, e.g. hydrostatic extrusion (HE).

The research aimed to analyze the anisotropy of the microstructure of the CuCrZr alloy and the resulting anisotropy of mechanical properties, depending on the direction of the research, after severe plastic deformation generated in the HE method. Earlier studies of this issue were conducted for the 6060-aluminum alloy, where higher strength values were observed in the direction longitudinal to the bar axis [27], or for grade 3 titanium, for which there was a difference in the crack character during small punch testing [28]. The occurrence of anisotropy in the CuCrZr alloy after the HE process has already been found in previous studies, but no microstructural and mechanical analyses depending on the direction of the study were performed [29]. However, its strong influence on the improvement of the service life of the produced electrodes for the spot-welding process from this material has been demonstrated.

2. MATERIALS AND METHODS

The tested material was the CuCrZr copper alloy with the chemical composition given in Table 1. From the point of view of the character of the research, the structure of the material in its initial state (before hydrostatic extrusion) needed to have an isotropic structure. The alloy was thus heat treated to obtain an isotropic structure on a transverse direction (TD) and longitudinal (LD) to the rod axis. The material was supersaturated at 1000°C for 1 hour and then cooled with water. This facilitated obtaining a single-phase, coarse-grained material (CG). Thanks to this, the research was conducted on an isotropic material, which is a reference to the changes taking place resulting from the anisotropy of the microstructure and properties as a function of deformation.

Table 1
Chemical composition of the CuCrZr alloy (in %)

Cr	Zr	Sb	Zn	Fe	P	Cu
0.7	0.08	0.01	0.01	0.03	0.01	balance

After the heat treatment process, the material was deformed according to the following procedure:

(a) The material in the form of bars with a diameter of 50 mm was subjected to a hydrostatic extrusion process with two different degrees of single deformation, with a reduction ratio of $R = 3.42$ and $R = 9.77$, where R is the ratio of the material sections before and after the extrusion process.

(b) The material in the form of a rod with a diameter of 35 mm was subjected to a single extrusion process with a reduction ratio of $R = 4.79$.

The parameters of the hydrostatic extrusion are given in Table 2.

Table 2
Size of plastic deformation in the process of hydrostatic extrusion of copper alloy CuCrZr

State	Reduction degree R	Actual deformation ε	Percentage deformation r %
Initial	1	0	0
$\phi 50 \rightarrow \phi 27$ mm	3.43	1.25	71
$\phi 35 \rightarrow \phi 16$ mm	4.79	1.57	79
$\phi 50 \rightarrow \phi 16$ mm	9.77	2.28	90

Hydrostatic extrusion was conducted on presses operating in the working pressure range up to 1.4 GPa, through a die with an apex angle of $2\alpha = 45^\circ$ in one extrusion operation at room temperature. In order to minimize the adiabatic heating effect during severe plastic deformation, the bars leaving the die were intensively cooled with cold running water. This allows us to minimize the grain growth process in the obtained material. The adiabatic heating effect is significant, especially in the HE process, which is characterized by high deformation rates under high-pressure conditions. The size of the adiabatic heating effect ΔT during HE is proportional to the extrusion pressure p and can be determined according to dependency (1) [30, 31]:

$$\Delta T = \beta(p/\rho c). \tag{1}$$

The methodology of the HE process has been described, inter alia, in [32, 33].

The structure of the material in its initial state and after plastic deformation was characterized on the basis of the following parameters:

- Average grain equivalent diameter d_{eq} (diameter is defined as the diameter of a circle with an area equal to the surface area of a given grain).
- Coefficient of variation CV (d_{eq}) defined as the ratio of the standard deviation to d_{eq}.
- Grain elongation coefficient α defined as the ratio of the mean maximum grain diameter to d_{eq}.

The grain sizes and shapes before and after the HE process were determined with the image analysis method using MicroMeter software [34]. These parameters were determined in over 100 randomly selected grains on the cross-section (perpendicular to the bar axis, TD) and longitudinal direction (parallel to the bar axis, LD). Microstructural observations for the initial material were conducted on the Nikon Eclipse LV150 optical microscope, and after plastic deformation on the FEI TECNAI G2 F20 transmission electron microscope. In both cases, the TD and LD sections of the bar were examined.

The microhardness measurements were conducted using an automated Zwick-Roell ZHV1-A hardness tester, with a load of 200 g during 15 s. The tests of mechanical properties were conducted on a Zwick/Roell Z250kN static testing machine with a constant speed of 0.008 s^{-1} on standardized fivefold macrospecimens with a diameter of 8 mm measuring part taken in the direction of extrusion. Mechanical measurements in both TD and LD sections of the bar extrusion were measured in a static

tensile test of mini samples with a width of 0.8 mm, a thickness of 0.6 mm, and a measuring part length of 5 mm on the ZWICK 780 machine. The dynamic impact tensile tests were carried out on an Instron Dynatup 9250HV drop hammer high-speed impact tester. On the TD section, the test was conducted according to the Charpy method in compliance with PN-EN ISO 148-1: 2010 standard on 10×10 mm samples with a U-shaped notch with a depth of 5 mm and a bottom rounding radius of 1 mm with an impact energy of 300 J. In the LD section, the impact tensile was conducted with an impact energy of 500 J on fivefold samples with geometry and a diameter of 8 mm. Both tests were conducted at room temperature with an impact speed of 4.7 m s^{-1}. The samples for impact tests were selected so that their active sections, taking an active part in cracking, were similar and amounted to 50 mm^2 (see Fig. 1).

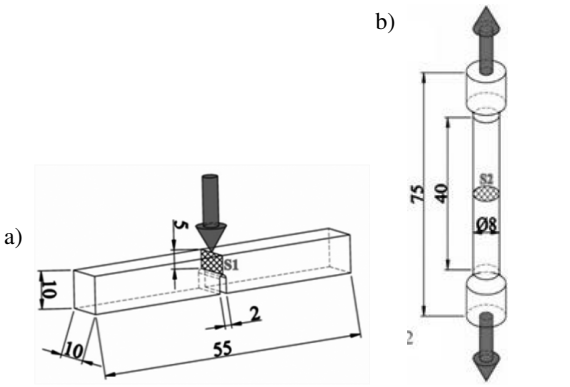

Fig. 1. Scheme and dimensions of samples for impact testing: a) by the Charpy method; b) by the impact tensile method

The impact strength tests conducted in the perpendicular direction by the Charpy method were determined as K_{CH}, and in the longitudinal direction by the impact tensile method, K_{IT} was determined. The percentage change in impact strength after the HE process from the isotropic value for the initial material was calculated according to the formula:

$$\Delta K_{\mathrm{CH,IT}} = \left[1 - \frac{K_{\mathrm{INIT(CH,IT)}}}{K_{\mathrm{CH,IT}}}\right] 100\%, \qquad (2)$$

where K_{CH} and K_{IT} – material impact strength measured by the Charpy method or the impact tensile method, K_{INIT} – impact strength of the initial material.

The calculated values allowed for the quantitative comparison of changes in impact strength on the cross-section and longitudinal section of the material after HE in relation to the isotropic initial material.

3. RESULTS AND DISCUSSION

3.1. Hydrostatic extrusion

The pressure characteristics of the HE process for the CuCrZr alloy for the three degrees of deformation ε used are shown in Fig. 2. The initial pressure increases show the compressibility of the pressure medium in the working chamber to a value that allows the extrusion process to be started. The pressure peaks are related to the onset of material extrusion and the associated change from static to kinetic friction. The subsequent flattening of the graphs indicates the stabilization of HE processes and the occurrence of plastic deformation at a constant extrusion speed. Final pressure drops correspond to the depressurization process of the working chamber. A constant and stable extrusion speed is important for uniform physical and mechanical properties over the entire length of the extruded product. The extrusion pressure of the copper alloy increased with the increase of the degree of deformation in the range between 500–700 MPa, Fig. 2. Higher extrusion pressure means greater mechanical work of plastic deformation, which is related to the higher temperature in the deformation zone of the material in the die (higher adiabatic heating).

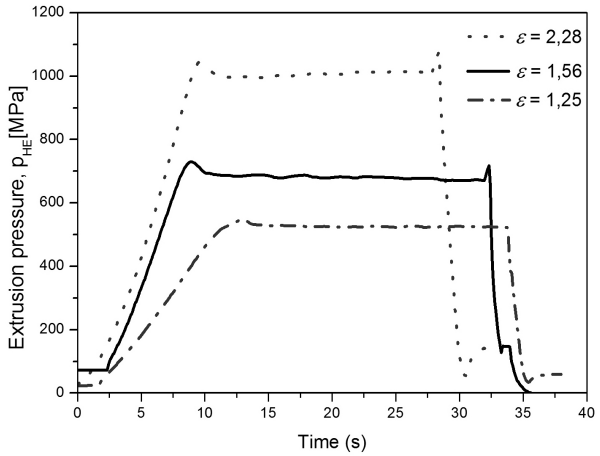

Fig. 2. Pressure characteristics of hydrostatic extrusion of CuCrZr copper alloy for three degrees of deformation

Assuming the density values for CuCrZr $\rho = 8.9$ gcm^{-3} and the specific heat $c = 0.386$ J g^{-1} K^{-1} and assuming the value $\beta 0.95$ in equation (1), the adiabatic heating effect ΔT in the range $\sim 132 - 258$°C, i.e. in the range of the homologous temperature $T_h = T/T_m = 0.12 - 0.24$ is obtained, where T is the estimated temperature and T_m is the melting point of the CuCrZr alloy, both in K degrees (see Table 3).

Table 3
Temperature of adiabatic heating during extrusion of the hydrostatic CuCrZr alloy. (a) The melting point of the CuCrZr alloy

ε	ΔT (°C)	$T_h = T/T_m^{(a)}$
1.25	132	0.12
1.57	172	0.16
2.28	258	0.24

$^{(a)}$ Melting temperature of CuCrZr $T_m = 1084$°C

3.2. Microstructure

From the point of view of the research objective, which was the analysis of structural anisotropy and mechanical properties after the hydrostatic extrusion process, it was important to obtain

the initial material with an isotropic structure. For this purpose, a heat treatment involving the supersaturation process was conducted. Figure 3 shows the microstructure of the CuCrZr alloy after supersaturation at 1000°C for one hour with cooling in water, on a section parallel (Fig. 3a) and perpendicular (Fig. 3b) to the bar axis.

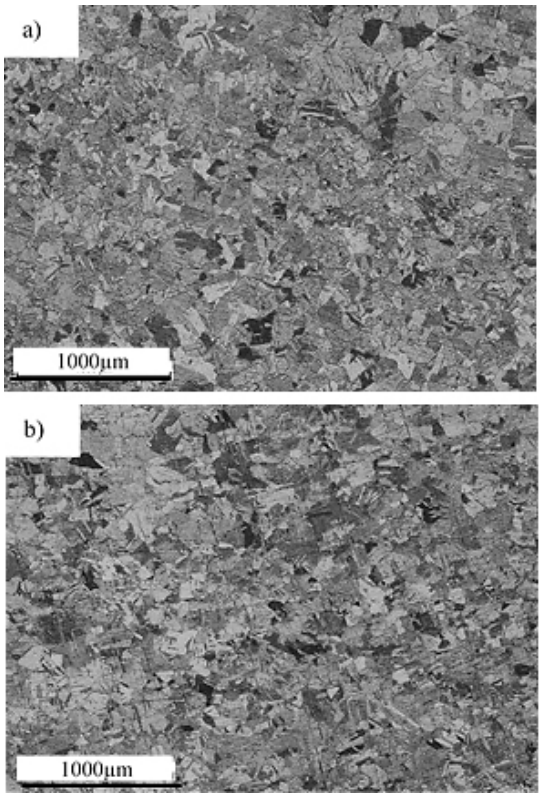

Fig. 3. Microstructure of the CuCrZr initial material after heattreatment (1000°C/1h/water): a) transverse section (TD);(b) longitudinal section (LD)

Both sections show a coarse-grained microstructure with multiple annealing twins. Based on the obtained values of the standard deviation SD (d_{eq}) $\sim$ 30 µm in both directions, it can be stated that the same grain sizes of $\sim$ 75 µm were obtained. The average coefficient of grain shape elongation for both sections was $\alpha \sim 1.4$. The similar α coefficients and the d_{eq} value for both sections prove that the structure is close to the isotropic state.

Hydrostatic extrusion causes a significant refinement of the structure, as shown in the images made with the TEM technique in Fig. 4. These observations revealed a characteristic microstructure with elongated grain bands on the LD section, which is particularly visible at the deformation $\varepsilon = 1.25$, $\varepsilon = 1.57$. At the highest degree of deformation, it can be noticed that this phenomenon begins to disappear and clear grains are observed Fig. 4e. This is also evidenced by the change in the character of the diffraction images (diffraction pattern SAED) shown for the TD direction, Fig. 4(a,c,e). For the actual deformation values $\varepsilon = 1.25$ and $\varepsilon = 1.57$, a clear structure of subgrains is observed in the areas of primary grains (single orientations), and at the highest deformation grains begin to form, as evidenced by a greater number of orientations in the SAED image. For all deformation degrees ε, a similar grain size/subgrain d_{eq} is observed on the cross-section in Table 4. The structure after hydrostatic extrusion is characterized by a high density of dislocations. The structure with high dislocation density is typical for copper alloys after SPD processes are subjected to relatively little deformation [35]. CuCrZr alloys are characterized by low stacking fault energy (SFE), as a result of which during plastic deformation dislocations are separated, which causes their greater cumulation. The dislocations overlap which, with further deformation, makes them behave like new dislocation sources.

Table 4
Sizes of the CuCrZr alloy grains after the hydrostatic extrusion process

True deformation ε	d_{eq} (PD) nm	d_{eq} (LD) nm
1.24	209	–
1.57	142	185
2.28	186	260

Figure 5 shows the grain size distributions of the CuCrZr alloy after successive extrusion stages and in the initial state. The measured sizes of the grains/subgrains ranged from 100 to 800 nm. The largest number of grains of $\sim$ 200 nm size was observed for all three degrees of deformation, at the level of approx. 40%. With the greatest degree of deformation $\varepsilon = 2.28$, a clear shift of their size towards larger grain sizes was observed. It can be caused by the strongest adiabatic heating effect, influencing the regrouping of microstructural defects and the formation of grains with higher disorientation angles through dynamic thermal processes occurring in the deformation zone. This is also evidenced by the previously discussed change in the character of diffraction images. More detailed information on the transformation of the microstructure with an increase in the degree of deformation was obtained by analyzing the measurements of the mean angles of material disorientation before and after HE (see Fig. 6). The classification proposed in [36] was adopted as a division criterion of the degree of grain boundary disorientation for the CuCrZr alloy, boundaries with a low disorientation angle are defined as having disorientation below 15°, low high-angle ranges from 15°–30°, medium-high ones within the range of 30°–45° and boundaries with a very high angle of disorientation between the grains of more than 45°. The initial material was characterized by mainly medium-high and very high disorientation angles. The greatest number was found in the range from 45° to 60°, but also grains with a small disorientation angle ($< 15°$), at the level of approx. 20%, could be observed.

After hydrostatic extrusion, this tendency was reversed and the boundaries with small disorientation angle had the greatest share in the material, regardless of the degree of deformation used. The share of such boundaries was between 70% and 75%. The decrease in the number of boundaries with a large disorientation angle at the deformation of $\varepsilon = 1.57$ compared to $\varepsilon = 1.25$ was related to the disappearance of the primary bound-

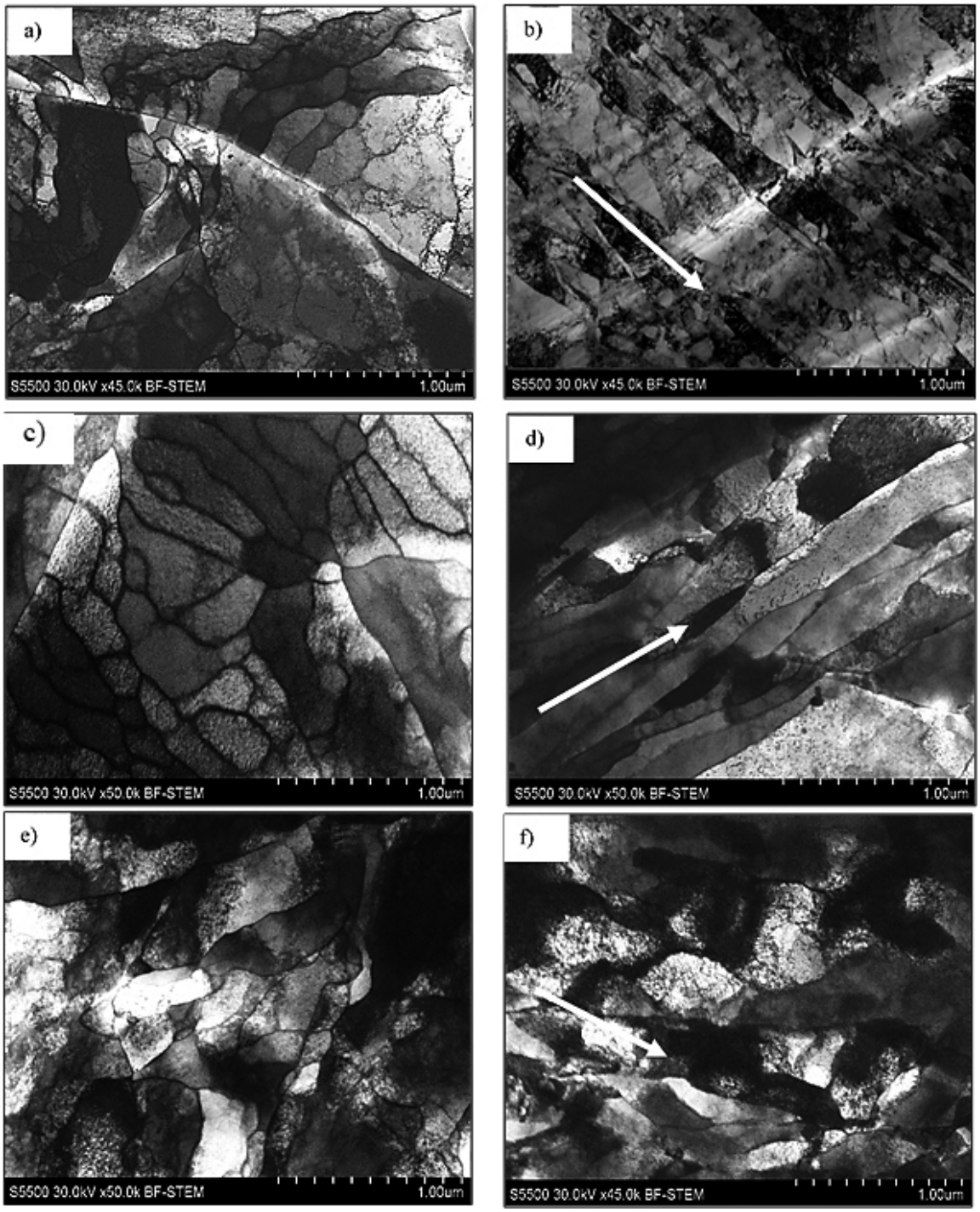

Fig. 4. TEM photos of the CuCrZr alloy after HE for different degrees of plastic deformation of the cross-section TD (a, c, e) and longitudinal LD (b, d, f). Deformations for (a, b), (c, d) and (e, f) respectively $\varepsilon = 1.25$, $\varepsilon = 1.57$, $\varepsilon = 2.28$. The arrows indicate the extrusion direction

aries in the material with increasing deformation. Growth at the maximum deformation $\varepsilon = 2.28$ is associated with the occurrence of heat-activated processes, healing, and dynamic recrystallization, as evidenced by the microstructural observation showing a clearly different character of the grains (Fig. 4). A similar dependence of the presence of a large number of grains with low angles in the CuCrZr alloy was also observed after plastic processing using the ECAP method [37].

The estimation of the anisotropic character of the microstructure was possible thanks to the analysis of the grain shape coefficient of the CuCrZr alloy, which showed that after the plastic deformation process, the greatest difference in grain character in both sections was observed at the lowest degree of deformation ($\varepsilon_{LD} = 2.09$ vs. $\varepsilon_{TD} = 1.47$) ~ 0.62, while for the initial material it was ~ 0.11 (Fig. 7). This difference resulted from the strongest effect of grain elongation on the longitudinal sec-

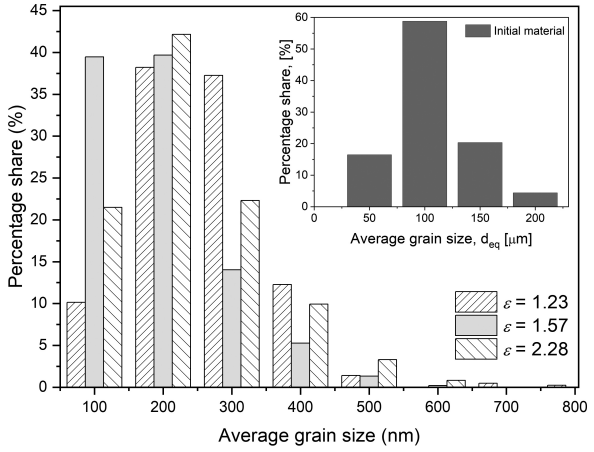

Fig. 5. The grain size distribution of the CuCrZr alloy in the initial state and after the hydrostatic extrusion process

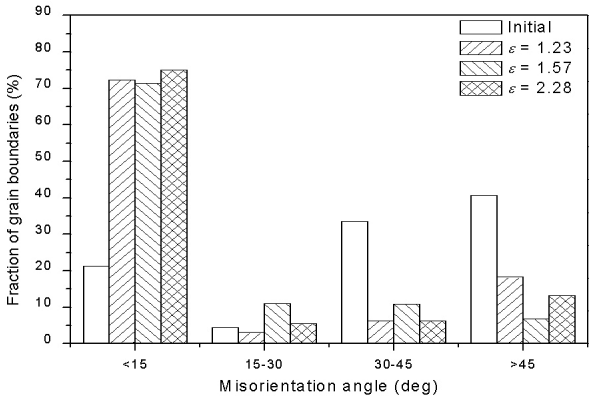

Fig. 6. Angles of grain disorientation in the CuCrZr copper alloy in the initial state and after the hydrostatic extrusion process

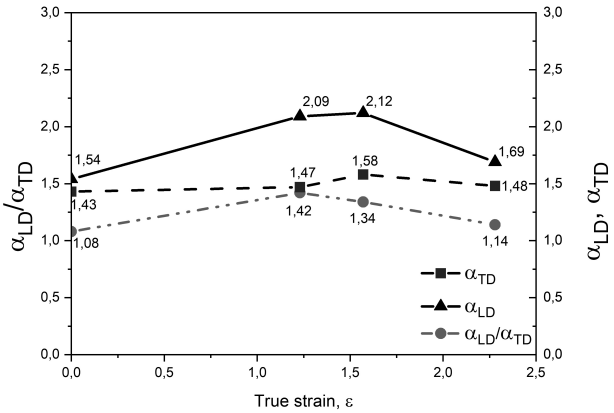

Fig. 7. Elongation of the grain shape and the ratio of the grain shape on the LD section to grains from the TD section in the CuCrZr alloy before and after plastic deformation using the HE method

tion. The ratio of the elongation of the grains on the LD section to the grains on the TD section, α_{LD}/α_{TD} in the initial material ~ 1 proves the similar character of the grain shape on both sections. The smallest differences in both sections, after the plastic deformation process, were observed with the application of the highest deformation degree $\varepsilon = 2.28$, where the grain shape coefficient was the lowest on the longitudinal section $\alpha_{LD} = 1.69$. Smaller differences in the character of the microstructure on both sections, for the highest degree of deformation, may be related to the specificity of plastic processing, for which the aforementioned strongest effects of adiabatic heating were observed under these conditions.

3.3. Mechanical properties

The anisotropy of the mechanical properties of the CuCrZr alloy is illustrated by the strength results made on mini samples in two perpendicular directions (Fig. 8).

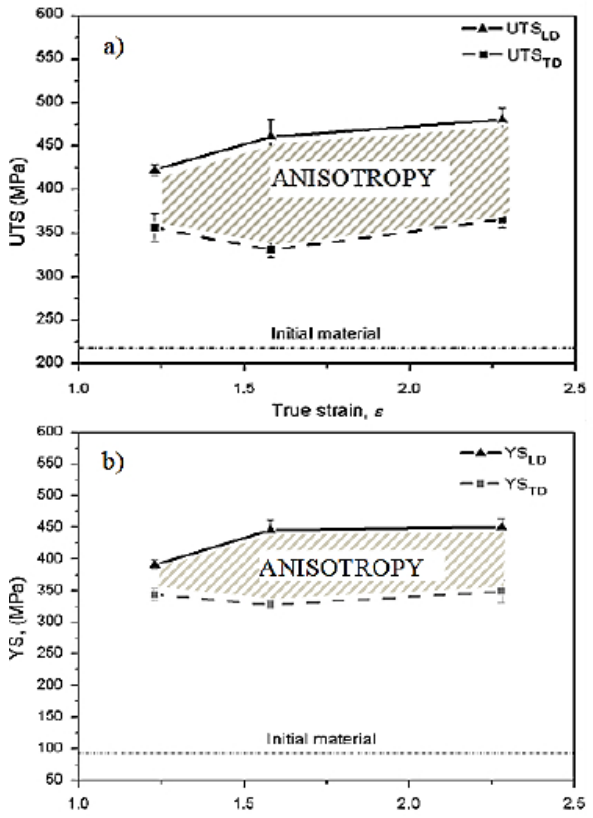

Fig. 8. Mechanical properties as a function of deformation from TD and LD sections of CuCrZr copper alloy after hydrostatic extrusion: (a) UTS and (b) YS

The measurement points are connected in the graph to better visualize the changes taking place. After the hydrostatic extrusion process for all deformation degrees in relation to CuCrZr in the initial state, the material strengthened in both sections. It is worth noting that changes in mechanical properties after hydrostatic extrusion on both sections (LD and TD) behave as in a typical commercial copper alloy CuCrZr after cold deformation and aging [38]. After the aging process, there is a significant increase in mechanical properties compared to the material in a supersaturated state. Both in the TD and LD section, the changes in the mechanical properties of UTS and YS, as a function of the actual deformation applied, are of a similar character, Fig. 8(a,b). In the LD section, both UTS and YS increase

as a function of the actual deformation, reaching the maximum values of 465 MPa and 470 MPa, respectively, but for the highest value of deformation, the increase is insignificant. In the TD section, both UTS and YS, with an average deformation value $\varepsilon = 1.57$, both measured values decrease, and with the greatest degree of deformation $\varepsilon = 2.28$, they slightly increase to the maximum values of 350 MPa and 360 MPa, respectively. The decrease in mechanical properties corresponds to the most strongly developed fibrous structure (Fig. 7). There are, however, significant differences in the measured values between the sections, which proves a clear effect of the anisotropy of mechanical properties after the extrusion process. In the TD section, lower UTS and YS values are observed across the entire range of deformations. The strongest anisotropy effect of mechanical properties depending on the research direction, both for tensile strength and yield strength, is observed at the deformation of $\varepsilon = 1.57$, where the most strongly developed fibrous structure was observed on the longitudinal section. The maximum differences in UTS and YS are 28% and 26%, respectively.

The anisotropy effect of the mechanical properties was also demonstrated by the hardness tests. For the CuCrZr alloy, the average value of the microhardness in the initial state in the cross-section and the longitudinal section was about 100 HV0.2 (Fig. 9). Regardless of the material plastic deformation procedure used, about a 50% increase in hardness is observed compared to the supersaturated material to the average value of 151 HV0.2 measured at the cross section. There are no clear changes in hardness depending on the applied degree of deformation. At the same time, the occurrence of hardness anisotropy of about 5% was observed, where higher values were obtained for the section perpendicular to the axis of the obtained bar. Similar differences between the values measured in both sections occur for all the applied degrees of deformation.

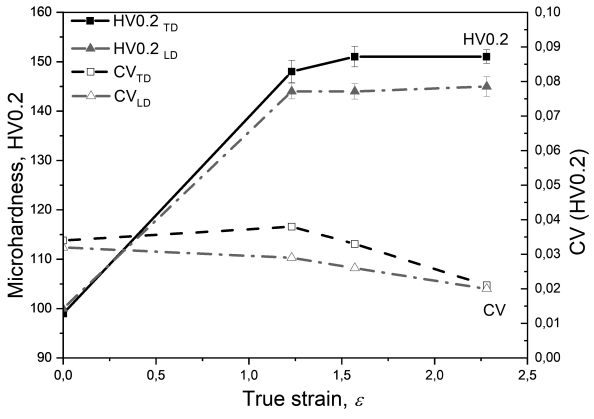

Fig. 9. Microhardness and CV in the initial material and after HE on TD and LD sections

These differences also appear in the coefficient of variation CV (HV0.2). With the increase of the actual deformation, its value decreases in both sections and at the highest degree of deformation, their values are similar. The reduction of CV (HV0.2) after the hydrostatic extrusion process indicates a better homogenization of the microstructure after HE. Homogenization after HE is characteristic of this method and was also observed in other materials, such as titanium and steel [32].

In order to determine the anisotropy of the material resistance to brittle fracture, depending on the direction of load application, the CuCrZr alloy was subjected to dynamic tests on a drop hammer in the Charpy and impact tensile tests. The results in the form of percentage changes in the impact strength with respect to the isotropic initial material as a function of the deformation degree are presented in Fig. 10.

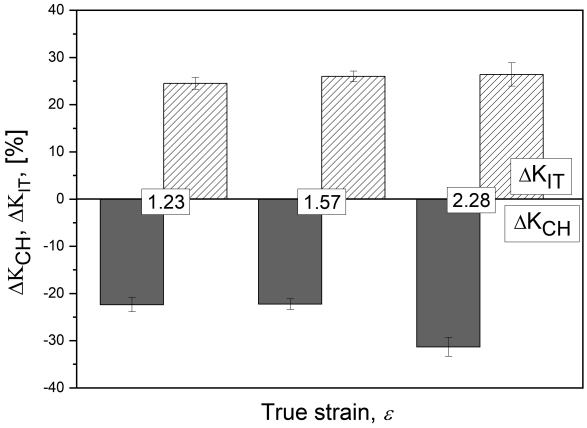

Fig. 10. Impact toughness variations for CuCrZr alloy after the HE process in transverse KCH and longitudinal K_{IT} cross-section with respect to the isotropic initial material K_{INIT} as the function of true strain ε

A clear anisotropy of impact strength was observed between the directions of load application during the impact tests. In the Charpy tests, where the force was applied perpendicular to the direction of the elongated grains, a decrease in impact strength was observed throughout the entire range of deformations. The material showed the greatest decrease in impact strength $\sim 30\%$ with the greatest degree of deformation ($\varepsilon = 2.28$). At two lower deformations, it showed a similar decrease of $\sim 20\%$. The obtained results can be commented on in comparison with the results of mechanical tests performed on mini-samples – Fig. 9a, where the increase in strength is observed with the highest degree of deformation in the cross-section. The dynamic impact strength tests, in which the test force was applied along the elongated grains, showed an increase in impact strength over the entire range of the applied strain rates at the level of $\sim 25\%$. The greatest increase in impact strength was observed for $\varepsilon = 2.28$. The increase in impact strength observed in the impact tensile tests indicates that the material tested under the load conditions applied along the elongated grains behaves like ultra-fine material, where an increase in impact strength was observed with a simultaneous increase in strength. Similar effects were observed in CuAl alloys after the cold rolling process [39, 40] and after the ECAP process [41, 42]. Under the conditions of impact load applied transversely to the direction of grain elongation, with a clear decrease in impact strength, changes characteristic of coarse-grained materials are observed and strength is accompanied by a decrease in impact strength.

4. CONCLUSIONS

The process of hydrostatic extrusion allowed us to obtain an ultra-fine-grained microstructure in the CuCrZr copper alloy for the applied plastic deformation degrees (average grain/subgrain size between $d_{eq} \sim 140$ nm and 200 nm).

Depending on the direction of the study, the microstructure showed a strong anisotropic character with elongated grains arranged parallel to the direction of the extrusion process. On the cross-section, the grains were similar to equiaxed grains.

With the highest degree of deformation $\varepsilon = 2.28$, as a result of strong thermal effects accompanying the HE process, the effects of the formation of a clear grain microstructure were observed, as evidenced by the character of SAED images, an increase in the average grain size, the share of grain boundaries with a large disorientation angle and changes in elongation coefficients.

After the HE process, the material obtained much higher mechanical properties compared to the initial material, but the anisotropy of the microstructure strongly influenced its character. Higher values of the yield point and tensile strength were obtained in the longitudinal section, where the force was applied parallel to the direction of extrusion and the elongation of the grains. The greatest differences in tensile strength were observed for the deformation $\varepsilon = 1.57$ at the level of $\sim 28\%$, for the yield point of $\sim 26\%$. At the same deformation value, the maximum mechanical properties were obtained, the UTS $= 460$ MPa and the YS $= 444$ MPa. For the highest value of the applied deformation, due to strong thermal effects and the decreasing effect of structural anisotropy in both directions of the research, the mechanical properties, and their differences were slightly reduced.

Similar relationships for the ultra-fine grained copper alloy CuCrZr were demonstrated after the ECAP process, where the material had an anisotropy of mechanical properties depending on the direction of the research [43]. However, this study did not analyze this phenomenon.

The anisotropy of properties depending on the research direction was also confirmed by hardness measurements, but the effect was not so clear. The occurrence of $\sim 5\%$ hardness anisotropy in the material after the HE process, where higher values were obtained for the section perpendicular to the axis of the obtained bar.

A clear anisotropy in the CuCrZr material after HE was demonstrated in the tests of the material resistance to dynamic loads. In the Charpy tests, where the load was applied perpendicularly to the direction of the elongated grains, a decrease in impact strength was observed in the entire range of deformations, and it was the highest ($\sim 30\%$) with the highest degree of deformation ($\varepsilon = 2.28$). The impact tests performed by dynamic tensile showed about a 25% increase in the impact strength, which was at a similar level in the entire range of the applied deformation degrees, which results from the typical ultra-fine-grained character of the microstructure in this section. On the other hand, in the Charpy test, the material behaved in a manner characteristic of coarse-grained materials.

The process of hydrostatic extrusion, due to its efficiency in grinding the microstructure and the possibility of producing large volumes of material, has a strong application potential, as demonstrated by, for example, previous studies conducted on the CuCrZr alloy for electrode applications in the spot-welding process [35]. The phenomenon of the formation of a characteristic microstructure after the HE process may determine the potential use of plastically processed materials. A detailed description of the phenomena of anisotropy of structural and mechanical properties after this process will allow for the optimal use of materials shaped by this technology.

REFERENCES

[1] R.Z. Valiev, A.P. Zhilyaev, and T.G. Langdon, *Bulk Nanostructured Materials. Fundamental and Applications*, TMS-Wiley, Hoboken, New Jersey, 2014, doi: 10.1002/9781118742679.

[2] M.Y. Murashkin, I. Sabirov, X. Sauvage, and R.Z. Valiev, "Nanostructured Al and Cu alloys with superior strength and electrical conductivity," *J. Mater. Sci. Lett.*, vol. 51, pp. 33–49, 2016, doi: 10.1007/s10853-015-9354-9.

[3] G. Purcek *et al.*, "Mechanical and wear properties of ultrafine-grained pure Ti produced by multi-pass equal-channel angular extrusion," *Mater. Sci. Eng. A*, vol. 517, pp. 97–104, 2009, doi: 10.1016/j.msea.2009.03.054.

[4] A. Kováčová *et al.*, "Investigation of the Ultrafine-Grained Structure Formation Under Different Strain Rates," *Arch. Metall. Mater.*, vol. 62, pp. 851–856, 2017, doi: 10.1515/amm-2017-0125.

[5] T. Kvackaj, A. Kovacova, R. Kocisko, J. Dutkiewicz, L. Litynska-Dobrzynska, and J. Kansy, "Relation between microstructural features and mechanical properties in oxygen free high conductivity copper after equal-channel angular pressing," *Kov. Mater.*, vol. 52, pp. 337–344, 2014, doi: 10.4149/km_2014_6_337.

[6] R. Valiev, "Nanostructuring of metals by severe plastic deformation for advanced properties," *Nature Mat.*, vol. 3, pp. 511–516, 2004, doi: 10.1038/nmat1180.

[7] I.J Beyerlein and L.S. Tóth, "Texture evolution in equal-channel angular extrusion," *Prog. Mater. Sci.*, vol. 54, 2009, pp. 427–510, doi: 10.1016/j.pmatsci.2009.01.001.

[8] R.Z. Valiev, R.K. Islamgaliev, and I.V. Alexandrov, "Bulk nanostructured materials from severe plastic deformation," *Prog. Mater. Sci*, vol. 45, no.2, pp. 103–189, 2000, doi: 10.1016/S0079-6425(99)00007-9.

[9] A. Vorhauer and R. Pippan, "On the homogeneity of deformation by high pressure torsion," *Scr. Mater,* vol. 51, no. 9, pp. 921–925, 2004, doi: 10.1016/j.scriptamat.2004.04.025.

[10] A.P. Zhilyaev and T.G. Langdon, "Using high-pressure torsion for metal processing: Fundamentals and applications," *Prog. Mater. Sci*, vol. 53, no. 6, pp. 893–979, 2008, doi: 10.1016/j.pmatsci.2008.03.002.

[11] B. Cherukuri, T.S. Nedkova, and R. Srinivasan, "A comparison of the properties of SPD processed AA-6061 by equal-channel angular pressing, multi-axial compressions/forgings and accumulative roll bonding," *Mater Sci Eng. A*, vol. 410–411, pp. 394–397, 2005.

[12] S. Lee., Y. Saito, T. Sakai, and H. Utsunomiya, "Microstructures and mechanical properties of 6061 aluminum alloy processed by accumulative roll-bonding," *Mater Sci Eng. A*, vol. 325, pp. 228–235, 2002, doi: 10.1016/S0921-5093(01)01416-2.

[13] O. Prakash and S. Sharma, "A review on accumulative roll bonding of severe plastic deformation process," *Int. J. Adv. Res. Innov. Ideas Educ.*, vol. 4, no. 3, pp. 2416–2435, 2018.

[14] J. Richert and M. Richert, "A new method for unlimited deformation of metals and alloys," *Aluminium*, vol. 62, no. 8, pp. 604–607, 1986.
[15] M. Kulczyk *et al.*, "Microstructure and mechanical properties of nickel deformed by hydrostatic extrusion," *Sci Mater*, vol. 22, no. 3, pp. 839–846, 2005.
[16] W. Pachla *et al.*, "Nanostructuring of metals by hydrostatic extrusion," *Conf. ESAFORM 2006*, 2006, pp. 535–538.
[17] M. Kulczyk, S. Przybysz, J. Skiba, and W. Pachla, "Severe plastic deformation induced in Al, Al-Si, Ag and Cu by hydrostatic extrusion," *Arch. Metall. Mater.,* vol. 59, no. 1, pp. 59–64, 2014, doi: 10.2478/amm-2014-0010.
[18] L. Sun, N.R. Tao, and K. Lu, "A high strength and high electrical conductivity bulk CuCrZr alloy with nanotwins," *Scr. Mater.,* vol. 99, pp. 73–76, 2015, doi: 10.1016/j.scriptamat.2014.11.032.
[19] Y.X. Tong, Y. Wang, Z. M. Qian, D.T. Zhang, L. Li, and Y.F. Zheng, "Achieving High Strength and High Electrical Conductivity in a CuCrZr Alloy Using Equal-Channel Angular Pressing," *Acta Metall. Sinica Engl.*, vol. 31, no. 10, pp. 1084–1088, 2018, doi: 10.1007/s40195-018-0766-9.
[20] H.T. Zhou, J.W. Zhong, X. Zhou, Z.K. Zhao, and Q.B. Li, "Microstructure and properties of Cu-1.0Cr-0.2Zr-0.03Fe alloy," *Mater. Sci. Eng. A*, vol. 498, no. 2, pp. 225–230, 2008, doi: 10.1016/j.msea.2008.07.061.
[21] V.I. Zeldovich, N. Yu. Frolova, I.V. Khomskaya, A.E. Kheifets, E.V. Shorokhov, and P.A. Nasonov, "Structure and microhardness of chromium–zirconium bronze subjected to severe plastic deformation by dynamic channel-angular pressing and rolling," *Phys. Met. Metall.*, vol. 115, pp. 465–470, 2014, doi: 10.1134/S0031918X14050159.
[22] R.K. Islamgaliev, K.M. Nesterov, and R.Z. Valiev, "Structure, strength, and electric conductivity of a Cu–Cr copper-based alloy subjected to severe plastic deformation," *Phys. Metals Metallogr.*, vol. 116, pp. 209–218, 2015, doi: 10.1134/S0031918X14090063.
[23] V.I. Zeldovich *et al.*, "Mechanical properties and the structure of chromium–zirconium bronze after dynamic channel-angular pressing and subsequent aging," *Phys. Metals Metallogr.,* vol. 117, pp. 74–82, 2016, doi: 10.1134/S0031918X16010129.
[24] I.S. Batra, G.K. Dey, U.D. Kulkarni, and S. Banerjee, "Precipitation in a Cu–Cr–Zr alloy," *Mater. Sci. Eng. A*, vol. 356, pp. 32–36, 2003, doi: 10.1016/S0921-5093(02)00852-3.
[25] V.R. Barabash, G.M. Kalinin, S.A. Fabritsiev and S.J. Zinkle, "Specification of Cu-Cr-Zr alloy properties after various thermomechanical treatments and design allowable including neutron irradiation effects," *J. Nucl. Mater.*, vol. 417, pp. 904–907, 2012, doi: 10.1016/j.jnucmat.2010.12.158.
[26] P. Lorenzetto *et al*., "EU R&D on the ITER First Wall," *Fusion Eng. Des. A*, vol. 81, pp. 355–360, 2006, doi: 10.1016/j.fusengdes.2005.07.040.
[27] S. Przybysz *et al*., "Anisotropy of mechanical and structural properties in AA 6060 aluminum alloy following hydrostatic extrusion process," *Bull. Polish Acad. Sci. Tech. Sci.*, vol. 67, no.4, pp. 709–717, doi: 10.24425/bpasts.2019.130180.
[28] E.C. Moreno-Valle *et al*., "Anisotropy of uniaxial and biaxial deformation behaviour of pure Titanium after hydrostatic extrusion," *Mater. Sci. Eng. A*, vol. 588, pp. 7–13, 2013, doi: 10.1016/j.msea.2013.08.044.
[29] H. Feng, H. Jiang, D. Yan, and L. Rong, "Effect of continuous extrusion on the microstructure and mechanical properties of a CuCrZr alloy," *Mater. Sci. Eng. A*, vol. 582, pp. 219–224, 2013, doi: 10.1016/j.msea.2013.06.031.
[30] I. Alexander, S.S. Pavlov and M. Kiritani, "Effective temperature rise during propagation of shock wave and high-speed deformation in metals," *Mater. Sci. Eng. A*, vol. 350, pp. 245–250, 2003, doi: 10.1016/S0921-5093(02)00711-6.
[31] F.K. Yan, G.Z. Liu, N.R. Tao, and K. Lu, "Strength and ductility of 316L austenitic stainless steel strengthened by nano-scale twin bundles," *Acta Mater.*, vol. 60, no. 3, pp. 1059–1071, 2012, doi: 10.1016/j.actamat.2011.11.009.
[32] W. Pachla, J. Skiba, M. Kulczyk, and M. Przybysz, "High-pressure equipment for cold severe plastic deformation working of materials," *Met. Form.*, vol. 26, no. 4, pp. 283–306, 2015.
[33] W. Pachla, M. Kulczyk, A. Mazur, and M. Sus-Ryszkowska, "UFG and nanocrystalline microstructures produced by hydrostatic extrusion of multifilament wires," *Int. J. Mater. Res.*, vol. 100, pp. 984–990, 2009, doi: 10.3139/146.110142.
[34] T. Wejrzanowski, W.L. Spychalski, K. Różniatowski, and K.J. Kurzydłowski, "Image based analysis of complex microstructures of engineering materials," *Int. J. Appl. Math. Comput. Sci.*, vol. 18, no. 1, pp. 33–39, 2008, doi: 10.2478/v10006-008-0003-1.
[35] M. Kulczyk *et al.*, "Improved compromise between the electrical conductivity and hardness of the thermo-mechanically treated CuCrZr alloy," *Mater. Sci. Eng. A*, vol. 724, pp. 45–52, 2018, doi: 10.1016/j.msea.2018.03.004.
[36] A. Vinogradov, Y. Suzuki, T. Ishida, K. Kitagawa, and V.I. Kopylov, "Effect of Chemical Composition on Structure and Properties of Ultrafine Grained Cu-Cr-Zr Alloys Produced by Equal-Channel Angular Pressing," *Mater. Trans.*, vol. 45, pp. 2187–2191, 2004, doi: 10.2320/matertrans.45.2187.
[37] A. Vinogradov, V. Patlan, Y. Suzuki, K. Kitagawa, and V.I. Kopylov, "Structure and properties of ultra-fine grain Cu–Cr–Zr alloy produced by equal-channel angular pressing," *Acta Mater.*, vol. 50, no. 7, pp. 1636–1651, 2002, doi: 10.1016/S1359-6454(01) 00437-2.
[38] Y.T. Zhu, T.C. Lowe, and T.G. Langdon, "Performance and applications of nanostructured materials produced by severe plastic deformation," *Scr. Mater.*, vol. 51, pp. 825–830, 2004, doi: 10.1016/j.scriptamat.2004.05.006.
[39] H. Li, Q. Q. Duan, and Z. F.Zhang, "Tearing toughness of ductile metals," *Acta Metall. Sin*., vol. 29, no. 2, pp. 150–155, 2016, doi: 10.1007/s40195-016-0371-8.
[40] P. Das, R. Jayaganthan, and I.V. Singh, "Tensile and impact-toughness behaviour of cryorolled Al 7075 alloy," *Mater. Des.*, vol. 32, no. 3, pp. 1298–1305, 2011, doi: 10.1016/j.matdes.2010.09.026.
[41] A. Sivaraman and U. Chakkingal, "Flow properties of commercial purity aluminum processed by equal channel angular pressing," *Mater. Sci. Eng. A.*, vol. 487, pp.264–270, 2008, doi: 10.1016/j.msea.2007.10.071.
[42] C. Xu, M. Furukawa, Z. Horita, and T.G. Langdon, "The evolution of homogeneity and grain refinement during equal-channel angular pressing: A model for grain refinement in ECAP," *Mater. Sci. Eng. A.*, vol. 398, pp. 66–76, 2005, doi: 10.1016/j.msea.2005.03.083.
[43] A. Vinogradov, "Fracture and fatigue resistance of ultrafine grain CuCrZr alloy produced ECAP," *Mater. Sci. Forum*, vol. 503–504, pp. 811–816, doi: 10.4028/www.scientific.net/MSF.503-504.811.